JACS
JOURNAL OF THE AMERICAN CHEMICAL SOCIETY

Communication

pubs.acs.org/JACS

An Intermetallic $Au_{24}Ag_{20}$ Superatom Nanocluster Stabilized by Labile Ligands

Yu Wang,[†] Haifeng Su,[†] Chaofa Xu,[†] Gang Li,[‡,§] Lars Gell,[∥] Shuichao Lin,[†] Zichao Tang,[‡] Hannu Häkkinen,[∥] and Nanfeng Zheng*[,†]

[†]State Key Laboratory for Physical Chemistry of Solid Surfaces, Collaborative Innovation Center of Chemistry for Energy Materials, and National Engineering Laboratory for Green Chemical Productions of Alcohols-Ethers-Esters, College of Chemistry and Chemical Engineering, Xiamen University, Xiamen 361005, China

[‡]State Key Laboratory of Molecular Reaction Dynamics, Dalian Institute of Chemical Physics, Chinese Academy of Sciences, Dalian 116023, China

[§]State Key Laboratory of Fine Chemicals, Institute of Coal Chemical Engineering, School of Chemical Engineering, Dalian University of Technology, Dalian 116012, China

[∥]Departments of Physics and Chemistry, Nanoscience Center, University of Jyväskylä, FI-40014 Jyväskylä, Finland

Supporting Information

ABSTRACT: An intermetallic nanocluster containing 44 metal atoms, $Au_{24}Ag_{20}(2\text{-SPy})_4(PhC{\equiv}C)_{20}Cl_2$, was successfully synthesized and structurally characterized by single-crystal analysis and density funtional theory computations. The 44 metal atoms in the cluster are arranged as a concentric three-shell $Au_{12}@Ag_{20}@Au_{12}$ Keplerate structure having a high symmetry. For the first time, the co-presence of three different types of anionic ligands (i.e., phenylalkynyl, 2-pyridylthiolate, and chloride) was revealed on the surface of metal nanoclusters. Similar to thiolates, alkynyls bind linearly to surface Au atoms using their σ-bonds, leading to the formation of two types of surface staple units ($PhC{\equiv}C\text{-Au-L}$, L = $PhC{\equiv}C^-$ or 2-pyridylthiolate) on the cluster. The co-presence of three different surface ligands allows the site-specific surface and functional modification of the cluster. The lability of $PhC{\equiv}C^-$ ligands on the cluster was demonstrated, making it possible to keep the metal core intact while removing partial surface capping. Moreover, it was found that ligand exchange on the cluster occurs easily to offer various derivatives with the same metal core but different surface functionality and thus different solubility.

Organic-capped metal nanoparticles represent an important class of nanomaterials that have found applications in catalysis, molecular sensing, electronics, and biology.[1−3] Surface capping agents not only help to stabilize nanoparticles against aggregation but also play an important role in surface functional modification of nanoparticles.[3−6] In the synthesis of metal nanoparticles, capping agents can be introduced in the forms of free ligands or ligands on metal precursors. However, it remains challenging to identify the detailed binding structure of capping agents on metal nanoparticles.[7−10] Owing to their truly monodisperse nature, atomically precise monolayer-protected metal nanoclusters have recently emerged as unique nanomaterials allowing the full characterization of their surface binding structures at the atomic level. With help from single-crystal X-ray crystallography, several important surface features on metal nanoparticles have been revealed.[7,11] For instance, with the resolution of a series of thiolated Au nanoclusters, "RS-Au-SR" staple units with Au atoms linearly bound by thiolates have been widely demonstrated as common surface binding motifs on thiolated Au nanoparticles.[11−17] Recently, studies have revealed that thiolated Ag,[18−21] AuAg,[20,22] and AuCu[23] nanoclusters could have non-staple units on their surfaces. The combined use of phosphine and thiolates provides an effective way to finely tune the distribution of surface Cu atoms on AuCu nanoclusters.[24]

Besides the structures that have been resolved by single-crystal analysis, a large number of pure organic-capped metal nanoclusters have been chemically prepared and characterized by other means.[25,26] The use of organic ligands having unique properties and structures has been demonstrated as an effective strategy to create new metal nanoclusters. In the case of Au nanoclusters, introducing bulky thiolates (e.g., S-Eind, 2,6-diphenylbenzenethiol) or thiolates capable of inter-ligand hydrogen bonding (*m*-mercaptobenzoic acid) helped to yield new Au clusters.[27−29] Although not prepared in thiolated forms, a series of new Au clusters were successfully synthesized when phenylalkynyl was used as the capping ligand.[30−34] Incorporating sulfide on the surface of thiolated Au nanoclusters introduced new surface capping structures.[35,36] However, there has been limited success in preparing Au nanoclusters having different types of ligands on their surfaces. It remains unaddressed whether labile surface ligands can be incorporated onto the same cluster and how they are bound on the surface. Addressing this issue is essential to creating functional clusters for applications.

We now report the first example of a metal nanocluster having three different types of anionic surface ligands: phenylalkynyl ($PhC{\equiv}C^-$, denoted as PA), 2-pyridylthiolate (PyS^-), and Cl^-. The cluster has an overall composition of $Au_{24}Ag_{20}(SPy)_4(PA)_{20}Cl_2$, with the 44 metal atoms distributed in a $Au_{12}@Ag_{20}@Au_{12}$ form having a concentric icosahedron@dodecahedron@

Received: February 4, 2015
Published: March 24, 2015

DOI: 10.1021/jacs.5b01232
J. Am. Chem. Soc. 2015, 137, 4324−4327

icosahedron three-shell Keplerate structure. Two different surface units (PhC≡C-Au-L, L = PhC≡C$^-$ or PyS$^-$) are revealed on the surface of the cluster, confirming that alkynyls are effective surface ligands to substitute thiolates for stabilizing Au nanoclusters.[30−34] Moreover, the presence of two Cl$^-$ on the cluster makes it possible to specifically modify its surface. Density funtional theory calculations show that the cluster has electronic structure with an 18-electron superatom shell closure. Replacing the four PyS$^-$ ligands by PA does not alter the optical properties of the cluster.

In a typical synthesis, $AuSMe_2Cl$ was first dissolved in the mixture solution of chloroform and methanol, after which $AgCH_3COO$ was added. The suspension was then cooled to 0 °C in an ice bath. After phenylacetylene and 2-pyridinethiol were added and stirred for 5 min, the reducing agent, *tert*-butylamine borane, was added to the mixture under vigorous stirring. The reaction was aged for 12 h at 0 °C. Solvents were removed through rotary evaporation, and the obtained products were re-dissolved into chloroform for crystallization. Black block crystals were obtained through slow solvent evaporation in a yield of ~40% (based on Au).

As revealed by single-crystal X-ray analysis, the obtained $Au_{24}Ag_{20}$ cluster is a neutral cluster with an overall composition of $Au_{24}Ag_{20}(SPy)_4(PA)_{20}Cl_2$ containing 44 noble-metal atoms (Figures 1a and S1). The metal framework of $Au_{24}Ag_{20}(SPy)_4(PA)_{20}Cl_2$ can be described as a concentric three-shell $Au_{12}@Ag_{20}@Au_{12}$ Keplerate structure (Figure 1b). The inner shell is a hollow icosahedral cage of Au_{12}. The Au atoms in the core Au_{12} shell have an average Au−Au bond length of 2.79 Å, slightly shorter than the Au−Au distance (2.884 Å) in bulk face-centered-cubic Au. The 20 Au_3 faces of the icosahedral Au_{12} cage are fully face-capped by Ag atoms to form the dodecahedral Ag_{20} shell. The Au−Ag distances between the inner Au_{12} shell and the Ag_{20} shell are averaged at 2.86 Å, indicating the strong metal bonding in the core two-metal shells. In the cluster, the 20 pentagonal Ag_5 faces of the dodecahedral Ag_{20} shell are further capped by another 12 Au atoms. Similar to the inner icosahedral Au_{12} cage, the 12 Au atoms in the outer shell are also arranged in an icosahedral form. However, no strong metal bonding between Au atoms (averaged Au−Au at 5.86 Å) is revealed in the outer Au_{12} complex shell. Therefore, the cluster should be better structurally described as an $Au_{12}@Ag_{20}$ core protected by a metal complex shell.

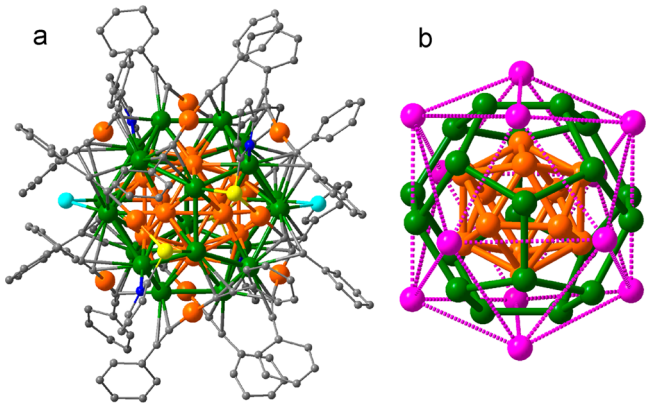

Figure 1. Crystal structure of the $Au_{24}Ag_{20}(SPy)_4(PA)_{20}Cl_2$ cluster. (a) Overall structure of the cluster. (b) Concentric three-shell $Au_{12}@Ag_{20}@Au_{12}$ framework of the 44 metal atoms in the cluster. Color legend: orange and pink spheres, Au; green sphere, Ag; yellow sphere, S; blue sphere, N; cyan sphere, Cl; gray sphere, C. All hydrogen atoms are omitted for clarity.

It should be noted that clusters containing 44 noble-metal atoms were first synthesized in a thiolated form in 2009 by Bakr, Stellacci, and co-workers.[37] The clusters were later identified to have a molecular formula of $[Ag_{44}(SR)_{30}]^{4-}$ using electrospray ionization mass spectrometry in 2012.[38] In 2013, the groups of Zheng and Bigioni determined the total structures of $[Ag_{44}(SR)_{30}]^{4-}$ clusters independently and revealed that each $[Ag_{44}(SR)_{30}]^{4-}$ cluster consists of a two-shell $Ag_{12}@Ag_{20}$ core.[20,21] The presence of the two-shell $M_{12}@M_{20}$ metal core is also found in thiolated $AuAg_{44}$ and $AuCu_{44}$ clusters,[20,22,23] and now in $Au_{24}Ag_{20}(SPy)_4(PA)_{20}Cl_2$.

The major difference between $Au_{24}Ag_{20}(SPy)_4(PA)_{20}Cl_2$ and previously reported thiolated Ag_{44}, $AuAg_{44}$, and $AuCu_{44}$ clusters lies in the arrangement of metal atoms in the outer metal complex shell. In fully thiolated clusters, the 12 metal atoms in the complex shell are present in the form of six $M_2(SR)_5$ (M= Cu, Ag) units connecting to six edges on the dodecahedral M_{20} shell. In sharp contrast, the 12 Au atoms in the outer complex shell in $Au_{24}Ag_{20}(SPy)_4(PA)_{20}Cl_2$ face-cap the 12 Ag_5 faces on the Ag_{20} shell. In total, there are 20 PhC≡C$^-$ ligands and 4 SPy ligands on the surface of each cluster. Every surface Au atom is linearly bound by two PhC≡C$^-$, or one PhC≡C$^-$ and one SPy ligands. Therefore, 12 "PhC≡C-Au-L" (L = PhC≡C$^-$, or PyS$^-$) staple units are found on the surface of each cluster.

Staple "RS-Au-SR" motifs are commonly revealed on the surface of thiolated Au nanoclusters and are typically bound to the inner metal atoms using their sulfur atoms. However, in $Au_{24}Ag_{20}(SPy)_4(PA)_{20}Cl_2$, the eight "PhC≡C-Au-C≡CPh" and the four "PhC≡C-Au-SPy" staple units one-to-one face-cap the 12 pentagonal Ag_5 faces on the Ag_{20} shell through C≡C and sulfur/pyridyl groups. Overall, as shown in Figure 2, the six

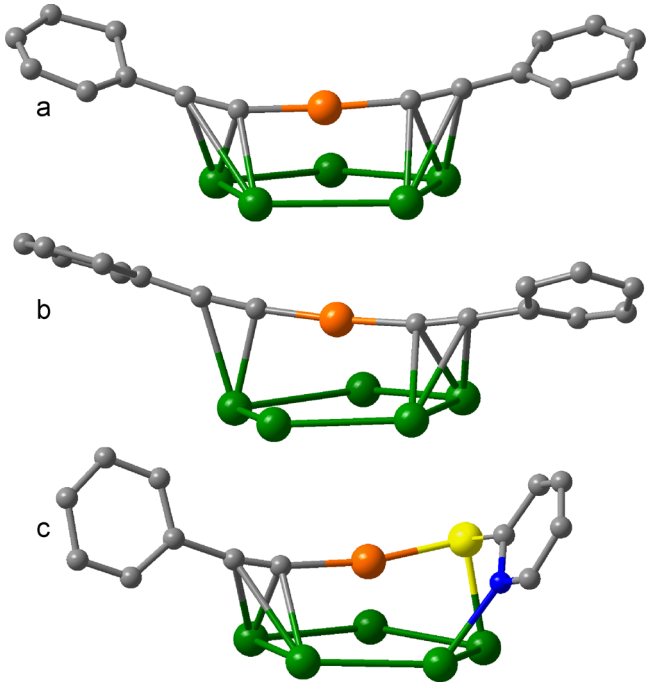

Figure 2. Three different binding structures of surface "PhC≡C-Au-L" staple units on Ag_5 faces of the Ag_{20} shell. Color legend: orange sphere, Au; green sphere, Ag; yellow sphere, S; blue sphere, N; gray sphere, C. All hydrogen atoms are omitted for clarity.

DOI: 10.1021/jacs.5b01232
J. Am. Chem. Soc. 2015, 137, 4324−4327

pairs of staple "PhC≡C-Au-L" motifs on the cluster display three different binding structures on Ag_5 faces. The 20 PhC≡C$^-$ ligands on the surface of the cluster exhibit several coordination modes, 16 as μ_3-η^1(Au),η^2(Ag),η^2(Ag) and four as μ_2-η^1(Au), η^2(Ag) ligands. The binding modes of PhC≡C$^-$ on Au and Ag revealed in $Au_{24}Ag_{20}(SPy)_4(PA)_{20}Cl_2$ have been widely documented in Au(I)/Ag(I) clusters.[39] Each PyS$^-$ ligand binds to two adjacent Ag atoms in the Ag_5 face with its S and Py moieties. Detailed bond lengths in the six pairs of staple "PhC≡C-Au-L" motifs on Ag_5 are illustrated in Figure S2.

Being able to incorporate three different anionic ligands in the same cluster is one of the prominent structural features in the $Au_{24}Ag_{20}$ cluster. Besides 20 PhC≡C$^-$ and 4 PyS$^-$ ligands, two Cl$^-$ anions are present on the surface of the cluster. They do not bind to the surface Au atoms, but serve as μ_2-ligands to bridge two adjacent Ag atoms on the Ag_{20} shell at the opposite positions of the cluster. With the presence of these two surface Cl$^-$ ligands, the cluster is neutral and capped by 26 mono-charged anionic ligands on its surface. According to the superatom model, the whole cluster has a shell-closing number of 18 valence electrons in the metal core.[40]

As shown in Figure 3a, the $Au_{24}Ag_{20}$ cluster exhibits a broad multiband optical absorption in the UV−vis region. Four

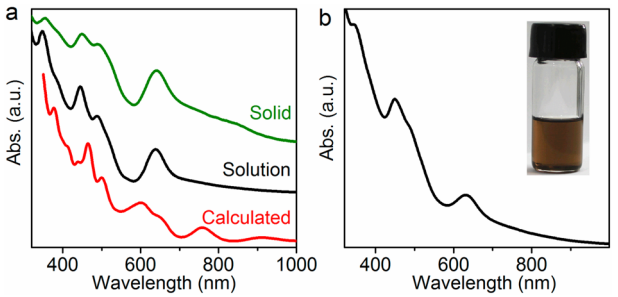

Figure 3. (a) Experimental and calculated optical absorption spectra of $Au_{24}Ag_{20}(SPy)_4(PA)_{20}Cl_2$. Absorption of clusters both in solid state and in solutions was measured. (b) Photograph showing the CH_2Cl_2 solution of the $Au_{24}Ag_{20}(SPy)_4(PA)_{20}Cl_2$ cluster after being heated in the solid-state form at 100 °C in air for 1 h and its optical spectrum.

apparent peaks (at 351, 447, 491, and 639 nm) and two shoulder peaks (at 381 and 513 nm) are observed. The optical gap of the cluster is estimated as 1.03 eV. The calculated spectrum reproduces these four features satisfactorily, even though slight shifts in the peak positions are observed. Analysis of angular momentum character of the frontier orbitals reveals clearly the 18-electron character of this cluster, with a set of five D-symmetric orbitals being the highest occupied ones and a set of seven F-symmetric and one S-symmetric (2S) orbitals spanning the first eight unoccupied states (Figure 4). This confirms that alkynyls work as electron-withdrawing ligands in the same way as thiolates and chlorides, as the metal atoms (Ag, Au) provide a total of 44 free electrons in the clusters, out of which 26 are withdrawn by the ligands (4 thiolates, 20 alkynyls, and 2 chlorides).

The crystal structure analysis on the cluster has clearly indicated the similarity of the binding structure of alkynyl and thiolate ligands on the surface of Au nanoclusters, consistent with recent theoretical and experimental studies.[34,41] It is thus structurally expected that the four thiolates on the cluster can be substituted by phenylalkynyls. Experimentally, we attempted to exclude the use of thiolates in the synthesis. As expected, the

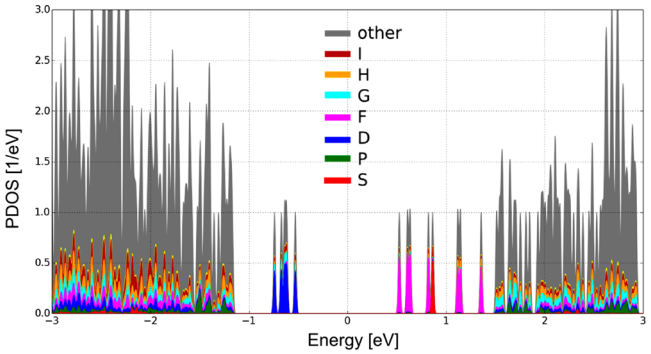

Figure 4. Angular momentum resolved projected density of states (PDOS) for $Au_{24}Ag_{20}(SPy)_4(PA)_{20}Cl_2$ cluster in the region of the HOMO−LUMO gap, centered around the Fermi energy at zero. The manifold of the highest occupied states consists of five superatomic 1D states (blue), and the first eight states above the HOMO−LUMO gap consist of seven superatomic 1F (purple) and one 2S (red) states. This analysis confirms that the cluster is an 18-electron superatom.

obtained cluster with no thiolates on its surface displays an optical absorption spectrum (Figure S3) similar to that of $Au_{24}Ag_{20}(SPy)_4(PA)_{20}Cl_2$. Moreover, the four 2-SPy$^-$ ligands on the cluster can also be substituted by four 2-SPyCOOH (6-mercaptonicotinic acid) to yield an alcohol-soluble $Au_{24}Ag_{20}$ cluster that exhibits the same optical absorption as $Au_{24}Ag_{20}(SPy)_4(PA)_{20}Cl_2$ (Figure S4). The two Cl$^-$ anions on the cluster are readily exchanged by thiolates (Figure S5), making it possible to yield the water-soluble $Au_{24}Ag_{20}$ cluster as well (Figure S6).

The presence of the three different types of surface ligands on $Au_{24}Ag_{20}(SPy)_4(PA)_{20}Cl_2$ makes it possible to selectively remove the surface ligands. Our temperature-programmed decomposition/mass spectrometric (TPD-MS) and thermogravimetric analysis (TGA) studies (Figures 5 and S7, also see

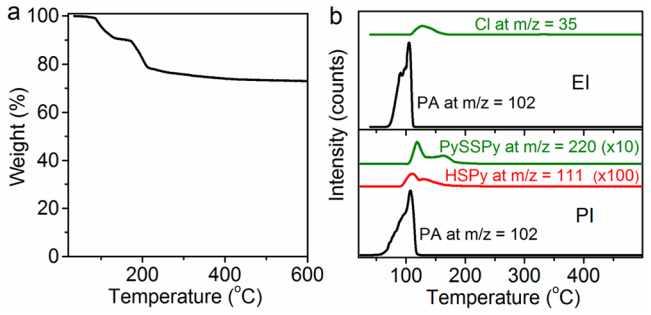

Figure 5. (a) TGA and (b) TPD-MS curves of the $Au_{24}Ag_{20}(SPy)_4(PA)_{20}Cl_2$ cluster. TGA was carried out by using N_2 as the carrier gas. TPD-MS spectra with both electron ionization (EI) and photon ionization (PI) modes are given.

Supporting Information for more details) clearly reveal that the release of PA from the cluster readily occurs below 100 °C. The cluster heated in the solid-state form at 100 °C in air for 1 h was still soluble in CH_2Cl_2. Major absorption peaks from its parental cluster were clearly observed in the optical spectrum of the treated sample (Figure 3b), while the clusters kept their particle size (Figure S8). Such a thermal behavior is distinct from that of reported thiolated metal nanoclusters in which the decomposition release of surface ligands often took place at temperatures above 150 °C.[16,24] The easy removal of PA at relatively low temperature makes it possible to keep the metal core of the cluster intact while partially removing the surface

DOI: 10.1021/jacs.5b01232
J. Am. Chem. Soc. 2015, 137, 4324−4327

ligands, which would be important to create catalytic sites on its surface.

In summary, an 18-electron AuAg intermetallic nanocluster, $Au_{24}Ag_{20}(SPy)_4(PA)_{20}Cl_2$, was synthesized and structurally determined. The structure of the cluster is unique in two aspects: (1) The metals are arranged in a three-shell Au_{12}@Ag_{20}@Au_{12} structure. (2) Three different anionic ligands are present on the surface of the cluster. Both PhC≡C$^-$ and PyS$^-$ ligands bind between the middle Ag_{20} shell and the outer Au_{12} shell, resulting in the formation of eight "PhC≡C-Au-C≡CPh" and four "PhC≡C-Au-SPy" staple units on the surface of the cluster. The bidentate feature of PhC≡C$^-$ and PyS$^-$ makes the surface structure of $Au_{24}Ag_{20}(SPy)_4(PA)_{20}Cl_2$ different from previously reported thiolated $[Au_{12}M_{32}(SR)_{30}]^{4-}$ (M = Ag or Cu) clusters. Upon thermal treatments, PhC≡C$^-$ ligands on the cluster are more labile than SPy$^-$ and Cl$^-$, making it possible to partially remove the surface capping agents at temperatures below 100 °C while keeping the metal core intact. Chemically, the anionic ligands on the cluster are readily ligand-exchanged to offer new functionality, such as solubility. We hope the demonstration of the labile feature of surface ligands in this work will stimulate work toward creating metal nanoclusters for catalytic and biological applications.

■ ASSOCIATED CONTENT

Supporting Information

Experimental details, detailed crystallographic data including the CIF file, computational details, analysis of the cluster electronic structure, TPD-MS measurements, mass spectra, and UV−vis spectra of clusters with different surface ligands. This material is available free of charge via the Internet at http://pubs.acs.org.

■ AUTHOR INFORMATION

Corresponding Author

*nfzheng@xmu.edu.cn

Notes

The authors declare no competing financial interest.

■ ACKNOWLEDGMENTS

We thank the MOST of China (2011CB932403, 2015CB932303) and the NSFC of China (21420102001, 21131005, 21390390, 21227001, 21333008) for financial support. Work at the University of Jyväskylä was supported by the Academy of Finland. The computations were made at the CSC computing center in Espoo, Finland, and at the HLRS center in Stuttgart, Germany.

■ REFERENCES

(1) Templeton, A. C.; Wuelfing, W. P.; Murray, R. W. *Acc. Chem. Res.* **1999**, *33*, 27.
(2) Niemeyer, C. M. *Angew. Chem., Int. Ed.* **2001**, *40*, 4128.
(3) Daniel, M.-C.; Astruc, D. *Chem. Rev.* **2003**, *104*, 293.
(4) Wu, B. H.; Zheng, N. F. *Nano Today* **2013**, *8*, 168.
(5) Niu, Z.; Li, Y. *Chem. Mater.* **2013**, *26*, 72.
(6) Verma, A.; Uzun, O.; Hu, Y.; Hu, Y.; Han, H.-S.; Watson, N.; Chen, S.; Irvine, D. J.; Stellacci, F. *Nat. Mater.* **2008**, *7*, 588.
(7) Häkkinen, H. *Nat. Chem.* **2012**, *4*, 443.
(8) Liu, X.; Yu, M.; Kim, H.; Mameli, M.; Stellacci, F. *Nat. Commun.* **2012**, *3*, 1182.
(9) Moglianetti, M.; Ong, Q. K.; Reguera, J.; Harkness, K. M.; Mameli, M.; Radulescu, A.; Kohlbrecher, J.; Jud, C.; Svergun, D. I.; Stellacci, F. *Chem. Sci.* **2014**, *5*, 1232.
(10) Ong, Q. K.; Reguera, J.; Silva, P. J.; Moglianetti, M.; Harkness, K.; Longobardi, M.; Mali, K. S.; Renner, C.; De Feyter, S.; Stellacci, F. *ACS Nano* **2013**, *7*, 8529.
(11) Jadzinsky, P. D.; Calero, G.; Ackerson, C. J.; Bushnell, D. A.; Kornberg, R. D. *Science* **2007**, *318*, 430.
(12) Zeng, C. J.; Li, T.; Das, A.; Rosi, N. L.; Jin, R. C. *J. Am. Chem. Soc.* **2013**, *135*, 10011.
(13) Qian, H. F.; Eckenhoff, W. T.; Zhu, Y.; Pintauer, T.; Jin, R. C. *J. Am. Chem. Soc.* **2010**, *132*, 8280.
(14) Heaven, M. W.; Dass, A.; White, P. S.; Holt, K. M.; Murray, R. W. *J. Am. Chem. Soc.* **2008**, *130*, 3754.
(15) Zhu, M. Z.; Aikens, C. M.; Hollander, F. J.; Schatz, G. C.; Jin, R. *J. Am. Chem. Soc.* **2008**, *130*, 5883.
(16) Zeng, C.; Qian, H.; Li, T.; Li, G.; Rosi, N. L.; Yoon, B.; Barnett, R. N.; Whetten, R. L.; Landman, U.; Jin, R. *Angew. Chem., Int. Ed.* **2012**, *51*, 13114.
(17) Jin, R. *Nanoscale* **2015**, *7*, 1549.
(18) Yang, H. Y.; Wang, Y.; Zheng, N. F. *Nanoscale* **2013**, *5*, 2674.
(19) Yang, H. Y.; Lei, J.; Wu, B. H.; Wang, Y.; Zhou, M.; Xia, A.; Zheng, L. S.; Zheng, N. F. *Chem. Commun.* **2013**, *49*, 300.
(20) Yang, H. Y.; Wang, Y.; Huang, H. Q.; Gell, L.; Lehtovaara, L.; Malola, S.; Häkkinen, H.; Zheng, N. F. *Nat. Commun.* **2013**, *4*, 2422.
(21) Desireddy, A.; Conn, B. E.; Guo, J.; Yoon, B.; Barnett, R. N.; Monahan, B. M.; Kirschbaum, K.; Griffith, W. P.; Whetten, R. L.; Landman, U.; Bigioni, T. P. *Nature* **2013**, *501*, 399.
(22) Zhang, X.; Yang, H. Y.; Zhao, X. J.; Wang, Y.; Zheng, N. F. *Chin. Chem. Lett.* **2014**, *25*, 839.
(23) Yang, H. Y.; Wang, Y.; Yan, J. Z.; Chen, X.; Zhang, X.; Häkkinen, H.; Zheng, N. F. *J. Am. Chem. Soc.* **2014**, *136*, 7197.
(24) Yang, H. Y.; Wang, Y.; Lei, J.; Shi, L.; Wu, X.; Makinen, V.; Lin, S. C.; Tang, Z.; He, J.; Häkkinen, H.; Zheng, L. S.; Zheng, N. F. *J. Am. Chem. Soc.* **2013**, *135*, 9568.
(25) Rao, T. U. B.; Pradeep, T. *Angew. Chem., Int. Ed.* **2010**, *49*, 3925.
(26) Udayabhaskararao, T.; Sun, Y.; Goswami, N.; Pal, S. K.; Balasubramanian, K.; Pradeep, T. *Angew. Chem., Int. Ed.* **2012**, *51*, 2155.
(27) Nishigaki, J.-i.; Tsunoyama, R.; Tsunoyama, H.; Ichikuni, N.; Yamazoe, S.; Negishi, Y.; Ito, M.; Matsuo, T.; Tamao, K.; Tsukuda, T. *J. Am. Chem. Soc.* **2012**, *134*, 14295.
(28) Nishigaki, J.-i.; Yamazoe, S.; Kohara, S.; Fujiwara, A.; Kurashige, W.; Negishi, Y.; Tsukuda, T. *Chem. Commun.* **2014**, *50*, 839.
(29) Azubel, M.; Koivisto, J.; Malola, S.; Bushnell, D.; Hura, G. L.; Koh, A. L.; Tsunoyama, H.; Tsukuda, T.; Pettersson, M.; Häkkinen, H. *Science* **2014**, *345*, 909.
(30) Maity, P.; Tsunoyama, H.; Yamauchi, M.; Xie, S.; Tsukuda, T. *J. Am. Chem. Soc.* **2011**, *133*, 20123.
(31) Maity, P.; Takano, S.; Yamazoe, S.; Wakabayashi, T.; Tsukuda, T. *J. Am. Chem. Soc.* **2013**, *135*, 9450.
(32) Maity, P.; Wakabayashi, T.; Ichikuni, N.; Tsunoyama, H.; Xie, S.; Yamauchi, M.; Tsukuda, T. *Chem. Commun.* **2012**, *48*, 6085.
(33) Yamazoe, S.; Koyasu, K.; Tsukuda, T. *Acc. Chem. Res.* **2014**, *47*, 816.
(34) Wan, X.-K.; Tang, Q.; Yuan, S.-F.; Jiang, D.-e.; Wang, Q.-M. *J. Am. Chem. Soc.* **2015**, *137*, 652.
(35) Yang, H. Y.; Wang, Y.; Edwards, A. J.; Yan, J. Z.; Zheng, N. F. *Chem. Commun.* **2014**, *50*, 14325.
(36) Crasto, D.; Malola, S.; Brosofsky, G.; Dass, A.; Häkkinen, H. *J. Am. Chem. Soc.* **2014**, *136*, 5000.
(37) Bakr, O. M.; Amendola, V.; Aikens, C. M.; Wenseleers, W.; Li, R.; Dal, N. L.; Schatz, G. C.; Stellacci, F. *Angew. Chem., Int. Ed.* **2009**, *48*, 5921.
(38) Harkness, K. M.; Tang, Y.; Dass, A.; Pan, J.; Kothalawala, N.; Reddy, V. J.; Cliffel, D. E.; Demeler, B.; Stellacci, F.; Bakr, O. M.; McLean, J. A. *Nanoscale* **2012**, *4*, 4269.
(39) Mak, T. C. W.; Zhao, L. *Chem.—Asian J.* **2007**, *2*, 456.
(40) Walter, M.; Akola, J.; Lopez-Acevedo, O.; Jadzinsky, P. D.; Calero, G.; Ackerson, C. J.; Whetten, R. L.; Gronbeck, H.; Häkkinen, H. *Proc. Natl. Acad. Sci. U.S.A.* **2008**, *105*, 9157.
(41) Tang, Q.; Jiang, D.-e. *J. Phys. Chem. C* **2015**, DOI: 10.1021/jp508883v.

DOI: 10.1021/jacs.5b01232
J. Am. Chem. Soc. 2015, 137, 4324−4327